

Clustering of Charged Inertial Particles in Turbulence

Jiang Lu, Hansen Nordsiek, Ewe Wei Saw,* and Raymond A. Shaw†

Department of Physics, Michigan Technological University, Houghton, Michigan 49931, USA
(Received 10 December 2009; revised manuscript received 9 March 2010; published 7 May 2010)

Holographic measurements of the clustering of electrically charged, inertial particles in homogenous and isotropic turbulent flow reveal novel particle dynamics. When particles are identically charged, Coulomb repulsion introduces a length scale below which inertial clustering is suppressed such that the radial distribution function (RDF) mimics that of a nonideal gas. The result is described with a Fokker-Planck framework modeling inertial clustering as a diffusion-drift process modified to include Coulomb interaction. The peak in the RDF is well predicted by the balance between the particle terminal velocity under Coulomb repulsion and a time-averaged “drift” velocity obtained from the nonuniform sampling of fluid strain and rotation due to finite particle inertia. The resulting functional form of the RDF matches the measurements closely, providing support for the drift-diffusion description of particle clustering.

DOI: 10.1103/PhysRevLett.104.184505

PACS numbers: 47.55.Kf, 47.27.Gs

Ordered (correlated, non-Poisson) spatial arrangements of charged particles are observed in colloids [1,2] and in “dusty plasmas” [3,4]. These systems exhibit complex dynamics and self-organization, and have been used as model systems for studies of fundamental processes in condensed matter, such as phase transitions. For example, radial distribution functions for charged particles demonstrate formation of “Wigner crystals” in colloids and phase transitions from Coulomb crystals to liquids and gases in dusty plasmas. At the simplest level the relative roles of the Coulomb interaction energy and the thermal energy kT can be expressed through the Bjerrum length scale, at which the two energies are equal. In this Letter we ask, how does the presence of unipolar charge influence the distribution of particles agitated, not by thermal energy, but rather by turbulence? In such a system charged particles interact through the Coulomb force, but simultaneously turbulence acts to randomize the particle positions. Furthermore, interactions between particles and the local fluid flow result in additional forces and therefore add the possibility of more complex dynamics.

Turbulent flows are known for their efficient mixing, which tends to stretch and deform “scalar fields” until gradients are sufficiently sharp that molecular diffusion leads to homogenization. Particles with finite inertia, however, are observed to “unmix” and form clusters that apparently favor regions of high strain and avoid regions of high vorticity [5,6]. The clustering is manifested as a power-law increase in the radial distribution function with decreasing scale, and an exponent that depends on the particle inertia [7–9]. If the particles are charged, the inertial forces tending to bring particles together therefore act against the Coulomb repulsion [10]. Besides the inherent interest in the turbulent dynamics of charged inertial particles, there are numerous applications of practical interest. The behavior of such particles is relevant to a variety of engineering processes and environ-

mental phenomena, from electrospray ionization to thunderstorms.

The dynamics of uncharged inertial particles are still a matter of some debate, but several theories link the power-law dependence of the radial distribution function for weakly inertial particles to a time-averaged drift velocity [8,11]. The drift can be understood by considering a turbulent flow with energy dissipation (Kolmogorov) length scale η containing particles of diameter $d \ll \eta$, and with particle mass density $\rho_p \gg \rho_f$ (subscripts p and f denote particle and fluid, respectively). In a reference frame at rest with one particle, the relative velocity of a neighboring particle separated by a distance r_i small compared to η (such that the flow can be considered smooth) can be approximated as $dw_i/dt = (\Gamma_{ij}r_j - w_i)/\tau_p$, where $dr_i/dt = w_i$ and $\Gamma_{ij} \equiv \partial u_i/\partial x_j$ is the fluid velocity gradient tensor [11]. The Stokes number is the ratio of the particle inertial response time and the Kolmogorov time, $St = \tau_p/\tau_\eta$. If particle inertia is weak, i.e., St is small, the particles nearly follow the motion of fluid elements, so r_i and w_i can be expanded as powers of St , ultimately resulting in a mean “drift velocity” $\langle w \rangle_p = -St[\langle \mathcal{S}^2 \rangle_p - \langle \mathcal{R}^2 \rangle_p]r/3\tau_\eta$, where \mathcal{S} and \mathcal{R} are dimensionless second invariants of the strain and rotation rate tensors, related to the velocity gradient tensor as $\tau_\eta^2 \Gamma_{ij} \Gamma_{jl} = \mathcal{S}^2 - \mathcal{R}^2$, and $\langle \cdot \rangle_p$ denotes average over particle paths. Because inertial particles tend to favor strain over rotation the drift is negative. Chun *et al.* [11] show that, in steady state, the radial distribution function $g(r)$ for particles of equal τ_p can be expressed as a balance between this inertial drift and turbulent diffusion tending to even out the spatial distribution:

$$0 = \frac{St}{3\tau_\eta} [\langle \mathcal{S}^2 \rangle_p - \langle \mathcal{R}^2 \rangle_p] r g + \mathcal{D} \frac{dg}{dr}, \quad (1)$$

where $\mathcal{D} \approx B_{nl} r^2/\tau_\eta$ is a “nonlocal” turbulent diffusivity

[12]. The balance results in a power-law form $g(r) = c_0(\eta/r)^{c_1}$, with $c_1 = (\text{St}/3B_{\text{nl}})[\langle S^2 \rangle_p - \langle \mathcal{R}^2 \rangle_p] = \langle w \rangle_p r / \mathcal{D}$. Essentially, c_1 is the ratio of the inward drift of particles due to finite inertia and an outward “drift” \mathcal{D}/r of particles due to turbulent diffusion. This power-law dependence is consistent with recent measurements [9,13,14].

The experimental system for the study of inertial particles in turbulence is described in detail elsewhere [15]. Briefly, it consists of a turbulence chamber, which is a 50-cm-side cube with a speaker-driven jet at each vertex [16]. The jets are driven with random, uncorrelated signals so as to generate turbulence that is approximately homogeneous and isotropic (measured by laser-Doppler velocimetry and 3D particle tracking). The root-mean-square velocity fluctuation u_{rms} , energy dissipation rate ε (determined via second-order longitudinal velocity structure functions from 3D particle tracking), Taylor-microscale Reynolds number R_λ , and Kolmogorov length scale $\eta = (\nu^3/\varepsilon)^{1/4}$ for the experiments are given in Table I. Particles of average diameter $d = 40 \mu\text{m}$ (dispersion $\approx \pm 5 \mu\text{m}$) are generated by a vibrating orifice, and are allowed to settle into the turbulent flow. Particle positions and velocity vectors are obtained using digital inline holography with subsequent digital reconstruction and three-dimensional particle tracking [15]. The optical system consists of a Nd:YLF laser, double-pulsed for velocimetry (20 ns pulse duration, 800 μs between two pulses, and 3 s between each pulse pair). The collimated beam is passed through a beam splitter and guided by mirrors through the center of the chamber and then directed onto two CCD cameras. The measurement volume, which is the region over which the two camera views overlap, is $36.1 \times 24.0 \times 36.1 \text{ mm}^3$.

Particle charging is a result of the generation process itself, with the magnitude being inversely related to the orifice size [17]. The net particle charge is determined by directing a horizontally aligned stream of particles between the plates of a parallel-plate capacitor. The particle trajectories bend and finally reach a “terminal velocity” perpendicular to the plates. The perpendicular component is measured by laser Doppler velocimetry and is easily

TABLE I. Turbulence, particle, and charge parameters for the four experiments. Experiments 1c and 1n are for charged and neutral particles, respectively, for a relatively low St. Experiments 2c and 2n are for charged and neutral particles, respectively, for a relatively high St.

	1c	1n	2c	2n
u_{rms} (cm s ⁻¹)	15	14	21	21
Re_λ	84	82	110	100
ε (W kg ⁻¹)	0.06	0.06	0.17	0.17
η (μm)	510	510	390	390
St	0.3	0.3	0.6	0.6
q (e)	380 000	~80 000	270 000	~60 000
r_* (mm)	1.7	~0.6	1.0	~0.4
$E_{\text{charge}}/E_{\text{turb}}$	2.0	~0.08	0.75	~0.04
$n^{-1/3}$ (mm)	10	7	12	7

related to the particle charge and diameter. The observed width of the charge distribution is accounted for by the width of the independently measured particle size distribution, confirming that the particle charge is uniform to within approximately 20 000 elementary charges. The particles typically have charges of several hundred thousand positive elementary charges each when produced from the orifice. When neutralized particles (reduced charge) are needed, negative ions are produced by corona discharge near the orifice, reducing particle charge by about a factor of 5.

Radial distribution functions for “neutral” and charged particles have been obtained for two Stokes numbers: one that has been shown in previous experimental work [14] to be in agreement with the theoretically predicted power law for $g(r)$, and a higher value to investigate departures from the $\text{St} \ll 1$ limit. The resulting radial distribution functions are shown in Fig. 1. The experimental conditions are summarized in Table I. Experiments are labeled as follows: low-St (low ε) charged and neutral are 1c and 1n, respectively; high-St (high ε) charged and neutral are 2c and 2n, respectively. The error bars displayed on the data curves represent the statistical sampling uncertainty.

The observed radial distribution functions for the “neutral” particles show power-law behavior in the dissipation range (scales $r \lesssim 10\eta$), and the exponents c_1 are in general agreement with previous experimental and theoretical work [11,13,14]. The radial distribution functions for the charged particles are qualitatively similar to that of a non-ideal gas: in the turbulent system considered here the particles experience short-range Coulomb repulsion and an effective attraction through their common interaction with the turbulent flow (the average drift into fluid regions of relative high strain). The balance between inertial drift and Coulomb repulsion, however, can be achieved only if particles are able to coexist within length scales on the order of the energy dissipation scale. In essence, the turbulence must be able to impart sufficient energy to the particles so as to disturb them from a Coulomb crystal or liquid arrangement. The particle spacing corresponding to such an arrangement is approximately $n^{-1/3}$, given in Table I, and is seen to be much greater than η . The electrostatic energy for particles separated by length scale η can be compared to the turbulent kinetic energy of particles separated by η , given in Table I as $E_{\text{charge}}/E_{\text{turb}}$, and this value is on the order of or less than unity for all experiments. These two facts together confirm that the “gas” state can be achieved and that inertial effects that operate in the dissipation range are accessible.

The influence of charge can be understood at a first level by including a Coulomb force term in the relative velocity equation

$$\frac{dw_i}{dt} = \frac{\Gamma_{ij}r_j - w_i}{\tau_p} + \frac{2}{m} \frac{kq^2\hat{r}_i}{r^2}, \quad (2)$$

where $k = 1/4\pi\epsilon_0$. We consider only pair interactions, as

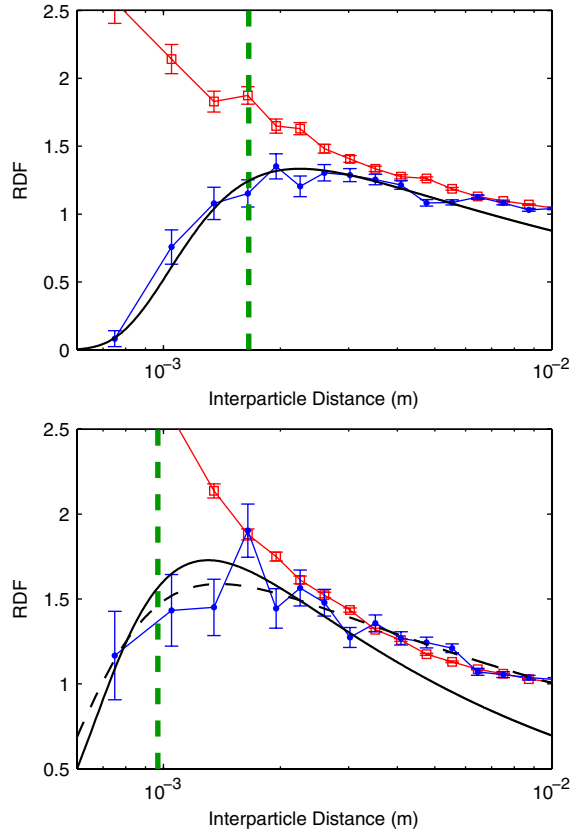


FIG. 1 (color online). Radial distribution functions for (top) $St \approx 0.3$ and (bottom) $St \approx 0.6$, showing results for both neutral (red squares) and charged (blue dots) particles. The green vertical dashed line denotes the scale r_* at which Coulomb and inertial drift forces are balanced for the charged particles. The solid and dashed black curves are the perturbation theory for inertia and charge effects [Eq. (4)], fitted to the experimental data (charged particles) within the dissipation range ($r \leq 10\eta$), for two fitting assumptions. First, c_1 was obtained from the corresponding neutral data and constrained while c_0 and c_2 were varied (solid curve). Second, all three parameters were varied (dashed curve). The dashed curve is not shown in the top panel because the two fitting methods resulted in essentially identical results. Fitting parameters for the $St \approx 0.3$ data are, in the order (c_0, c_1, c_2) , neutral: (2.7, 0.36, NA); charged with c_1 constrained: (2.6, 0.36, 15.5); charged with c_1 varied: (2.9, 0.44, 16.1). For the $St \approx 0.6$ data the parameters are as follows, neutral: (4.2, 0.53, NA); charged with c_1 constrained: (3.9, 0.53, 15); charged with c_1 varied: (2.5, 0.28, 10).

is reasonable for the dilute suspensions considered here. Furthermore, the absence of ions implies that there are no significant screening (Debye) effects, as, for example, exist in dusty plasmas [4]. This ultimately leads to a modified drift velocity $\langle w \rangle_p = -St[\langle \mathcal{S}^2 \rangle_p - \langle \mathcal{R}^2 \rangle_p]r/3\tau_\eta + St\tau_\eta 2kq^2/mr^2$. The relative particle velocity now results from an inward inertial drift and an outward Coulomb drift (at the peak of $g(r)$ turbulent diffusion can be neglected). We may expect that the scale r_* at which $\langle w \rangle_p = 0$ should correspond approximately to the peak of the radial distribution function. We use c_1 to infer the relative sampling of

strain and rotation for inertial particles, thereby obtaining $r_* = (2kq^2\tau_\eta\tau_p/mB_{nl}c_1)^{1/3}$. Using the value of c_1 determined from the neutral data, the balance scale can be calculated; the results are given in Table I and are denoted in Fig. 1 by the vertical dashed lines. There is reasonable agreement between the calculated r_* and the peak in $g(r)$ for the charged particles. At the same time, the calculated r_* for neutral (weakly charged) particles is so small as to be beyond the spatial resolution of our measurements, consistent with the observed $g(r)$.

A more complete expression for $g(r)$ can be obtained by including the new Coulomb drift term in the Fokker-Planck equation for particle-separation probability [proportional to $g(r)$]. The modified relative velocity is $w_i = \Gamma_{ij}r_j - St[\langle \mathcal{S}^2 \rangle_p - \langle \mathcal{R}^2 \rangle_p]r_i/\tau_\eta + 2kq^2\hat{r}_i St\tau_\eta/mr^2 = w_{\text{original}} + w_{\text{charge}}$. We then follow the derivation of Chun *et al.* [11] with the additional term $\langle w_{\text{charge}} \rangle$ to obtain an equation for $\partial g(r, t)/\partial t$ and finally take the steady-state limit to obtain an ODE analogous to Eq. (1):

$$0 = \frac{St}{3\tau_\eta}[\langle \mathcal{S}^2 \rangle_p - \langle \mathcal{R}^2 \rangle_p]rg + St\tau_\eta \frac{2kq^2}{mr^2}g + \mathcal{D} \frac{dg}{dr}, \quad (3)$$

based on the assumption that multiparticle (greater than two) Coulomb interactions are negligible. The solution including the charge influence is

$$\begin{aligned} g(r) &= c_0 \left(\frac{\eta}{r}\right)^{c_1} \exp\left[-\frac{2}{3B_{nl}}\tau_\eta\tau_p\left(\frac{kq^2}{m}\right)\left(\frac{1}{r^3}\right)\right] \\ &= c_0 \left(\frac{\eta}{r}\right)^{c_1} \exp\left[-c_2 St \left(\frac{E_{\text{charge}}}{E_{\text{turb}}}\right)\left(\frac{\eta}{r}\right)^3\right], \quad (4) \end{aligned}$$

where $c_2 = 2/3B_{nl}$, again with B_{nl} being the dimensionless coefficient for turbulent diffusivity. In the last expression, $E_{\text{charge}} = kq^2/m\eta$ is the energy of the Coulomb interaction at the dissipation scale and $E_{\text{turb}} = (\eta/\tau_\eta)^2$ is the energy of the Kolmogorov eddies. This exponent apparently has the same functional dependence as that derived independently by Alipchenkov *et al.* [10] for $St \ll 1$, in the limit of infinite Debye screening length, although the exact numerical coefficients are difficult to evaluate. The dependence of this energy ratio, which may be called the Coulomb number, on experimentally controllable variables is $q^2\varepsilon^{1/4}/d^3\rho_p\nu^{7/4}$, and the values for our experiments are given in Table I.

Finally, insight can be gained by writing the charge term as $\exp(-2v_{\text{charge}}/3v_{\text{turb}})$, where v_{charge} is the “terminal speed” of a particle due to the Coulomb interaction, and $v_{\text{turb}} = \mathcal{D}/r$ is a turbulent diffusion speed. Thus, it is explicitly seen that the exponential term neglects direct coupling between Coulomb and inertial effects, the two interacting only indirectly through the turbulent diffusivity. This is further evident in Eq. (4), which is a product of radial distribution functions for inertial clustering and for Coulomb interactions: $g_{\text{total}} = g_{\text{inertia}}g_{\text{charge}}$. It is a consequence of the logarithmic form of the governing differen-

tial equation and our assumption that the two drift velocities are independent. Effectively, we have not only neglected interactions beyond pair-interactions in the Coulomb term, but we have assumed that Coulomb interactions do not significantly alter the weak particle-fluid decoupling required to obtain expressions for inertial drift and turbulent diffusion (i.e., the terms that enter c_1).

The experimental results can be compared to the theory in a phenomenological way by fitting the “constants” c_0 , c_1 , and c_2 in Eq. (4). The resulting functions are shown in Fig. 1, with the fitting parameters given in the caption. First, we note that c_0 is not of primary interest here, because it is not determined by the theory, depending on the transition from dissipation to inertial range and perhaps on the data normalization [14]. Second, the c_1 for the neutral particles are somewhat less than obtained from simulations, consistent with the effects of size dispersion (e.g., see Sec. 6.2.2 of [14]) and with the effects of gravitational sedimentation. The fitting of the charged data was accomplished in two ways: constraining c_1 to be the value obtained from the corresponding neutral data, and fitting of all three parameters. The results of the two fitting methods for the charged data, constrained c_1 versus varied c_1 (described in the figure caption) allow us to draw several conclusions. First, the results for the low-St data (charged and neutral) are statistically identical, confirming the assumption that inertial drift and Coulomb interactions can be treated independently. Second, c_2 obtained for the low-St and the high-St data, with c_1 constrained, are statistically identical. The c_2 are 2.1 and 2.2 times the theoretical value $2/3B_{nl}$, respectively, with B_{nl} taken from [11]. We consider the agreement between experiments to be highly encouraging in validating the theory. The consistent offset may be a result of multiparticle Coulomb interactions, a supposition that can be tested by varying the particle number density. Third, for the charged, high-St data, the constrained and unconstrained fitting procedures yield different c_1 and c_2 . Specifically, c_1 drops by nearly a factor of 2 when unconstrained, and c_2 drops by 30%. Neither fit is statistically favored so it is premature to draw solid conclusions. Both reductions, however, would be consistent with an increase in the turbulent diffusivity \mathcal{D} , perhaps due to coupling between the Coulomb dispersion and particle inertial sampling of the turbulence, currently unaccounted for in the theory.

To summarize, we have measured the clustering of electrically charged, inertial particles in nearly homogeneous and isotropic turbulent flow. When particles are identically charged, Coulomb repulsion introduces a scale below which inertial clustering is suppressed. The result can be described with a Fokker-Planck framework, which models inertial clustering as a diffusion-drift process, modified to include Coulomb interaction. This results in a functional form for the radial distribution function that matches the measurements closely. This work provides

strong support for the utility of the Fokker-Planck framework [11] and the hypothesized drift-diffusion mechanism of particle clustering. Perhaps most intriguing for the future is the feasibility of using charged particles for probing the dynamical properties of particles in turbulence, and even the turbulent flow itself. On the practical side, the results have implications for collisions of charged particles in turbulence: a reduced radial distribution function at small scales, resulting from Coulomb repulsion, will tend to reduce the collision probability [7].

This work was supported by the U.S. National Science Foundation (Grant No. ATM-0535488). This work was carried out in cooperation with the International Collaboration for Turbulence Research.

*Present address: Max Planck Institute for Dynamics and Self Organization, Göttingen, Germany.

†rashaw@mtu.edu

- [1] W.B. Russel, D.A. Saville, and W.R. Schowalter, *Colloidal Dispersions* (Cambridge, Cambridge, U.K., 1989).
- [2] E.B. Sirota, H.D. Ou-Yang, S.K. Sinha, P.M. Chaikin, J.D. Axe, and Y. Fujii, *Phys. Rev. Lett.* **62**, 1524 (1989).
- [3] J.H. Chu and Lin I, *Phys. Rev. Lett.* **72**, 4009 (1994).
- [4] V.E. Fortov *et al.*, *Phys. Rev. Lett.* **90**, 245005 (2003).
- [5] J.K. Eaton and J.R. Fessler, *Int. J. Multiphase Flow* **20**, 169 (1994).
- [6] S. Sundaram and L.R. Collins, *J. Fluid Mech.* **335**, 75 (1997).
- [7] W.C. Reade and L.R. Collins, *Phys. Fluids* **12**, 2530 (2000).
- [8] G. Falkovich, A. Fouxon, and M.G. Stepanov, *Nature (London)* **419**, 151 (2002).
- [9] E.W. Saw, R.A. Shaw, S. Ayyalasomayajula, P.Y. Chuang, and A. Gylfason, *Phys. Rev. Lett.* **100**, 214501 (2008).
- [10] V.M. Alipchenkov, L.I. Zaichik, and O.F. Petrov, *High Temp.* **42**, 919 (2004).
- [11] J. Chun, D.L. Koch, S.L. Rani, A. Ahluwalia, and L.R. Collins, *J. Fluid Mech.* **536**, 219 (2005).
- [12] Nonlocal implies that the diffusive flux depends on pair probabilities at two distinct particle positions, as a result of long temporal correlations that lead to relative particle displacements of the same order as initial separation. Note that, where possible, we have used the notation of Chun *et al.* [11].
- [13] J.P.L.C. Salazar, J.D. Jong, L. Cao, S.H. Woodward, H. Meng, and L.R. Collins, *J. Fluid Mech.* **600**, 245 (2008).
- [14] E.W. Saw, Ph.D. thesis, Michigan Technological University, 2008.
- [15] J. Lu, J.P. Fugal, H. Nordsiek, E.W. Saw, R.A. Shaw, and W. Yang, *New J. Phys.* **10**, 125013 (2008).
- [16] W. Hwang and J.K. Eaton, *Exp. Fluids* **36**, 444 (2004).
- [17] A.G. Bailey, *Electrostatic Spraying of Liquids* (John Wiley & Sons, New York, 1988).